The Use of Electrical Conductivity and Magnetic Susceptibility Tensors in Rock Fabric Studies

D. A. Clark
CSIRO Div. of Mineral Physics and Mineralogy
P.O. Box 136
North Ryde NSW 2113

D. W. Emerson
Dept. Geology and Geophysics
University of Sydney
NSW 2006

T. L. Kerr
BHP Exploration
695 Burke Rd
Camberwell
Vic. 3124

Summary

Laboratory electrical conductivity (σ) anisotropy measurements were made on water saturated Palaeozoic black shales, mineralized schists, and banded and massive sulphides from the Mt Lyell region Tasmania. Macro- and micro-fabric and magnetic anisotropy studies were also carried out. Directional 1 kHz conductivity values were obtained in 9 directions for each of 10 samples. Reduction of these measurements produced the electrical conductivity tensor principal values and directions which were correlated with the fabric and magnetic data. The study suggests that: (i) a water saturated layered rock may be characterised by large $\sigma_1{:}\sigma_2{:}\sigma_3$ anisotropy; (ii) the conductivity tensor representation may reflect petrofabric; and (iii) anisotropy may cause the current density to deflect significantly from the electric field direction.

Introduction

Electrical conductivity (σ) and magnetic susceptibility (k) anisotropies are quite common in igneous, metamorphic, and sedimentary rocks and in sulphide and oxide ores. The anisotropy is usually ignored with these important petrophysical quantities being treated as scalars where magnitude only is considered. Anisotropy implies directional effects with the response vectors, current density $\tilde{J}_{cd}$ or magnetisation $\tilde{J}_{mag}$, being related to the stimulus vectors, electric field $\tilde{E}$ or magnetic field $\tilde{F}$, by second rank symmetric tensors ($\sigma_{ij} = \sigma_{ji}$, $k_{ij} = k_{ji}$) described by an array of 3^2 physical quantity components of which six are independent. For the electrical case $\tilde{J}_i = \sigma_{ij}\tilde{E}_j$ (i,j = 1,2,3) giving, by the Einstein summation convention (Nye, 1964), for orthogonal axes x_1, x_2, x_3:

$$J_1 = \sigma_{11}E_1 + \sigma_{12}E_2 + \sigma_{13}E_3$$
$$J_2 = \sigma_{21}E_2 + \sigma_{22}E_2 + \sigma_{23}E_3$$
$$J_3 = \sigma_{31}E_3 + \sigma_{32}E_2 + \sigma_{33}E_3$$

The tensor natures of conductivity and susceptibility may be studied in the laboratory by directional measurements in at least six orientations. Usually nine orientations are measured to permit error estimates. In rock magnetism data from commercially available susceptibility delineations have been used widely in fabric studies (e.g. see: Bhathal, 1971; Noltimier, 1971; Hrouda, 1973). In electrical petrophysics the little work that has been done appears to have been confined to permittivity studies of dry rocks (e.g. Hill, 1972).

Some of the basic aspects of anisotropy and fabric are summarised in Figs. 1 and 2 and Table 1. Neumann's Principle (Nye, 1957) states that a physical-property symmetry *includes* the geometric fabric symmetry. The symmetries are not necessarily the same as can be seen in Table 1 where monoclinic and triclinic petrofabrics manifest a higher (orthorhombic) physical property symmetry.

Laboratory Measurements

The conductivity anisotropies of water saturated mineralized rocks from northwest Tasmania were investigated in the Petrophysics Laboratory at the University of Sydney (Kerr, 1986) where micro- and macro-fabric observations and density/porosity determinations were also made. The test rock suite comprised disseminated, banded, and massive sulphides and black shales mainly from Mt Lyell. Magnetic anisotropy measurements were carried out on a Digico delineator in the CSIRO Mineral Physics Magnetics Laboratory at North Ryde. The main purpose of the study was to determine the conductivity characteristics; the magnetic and visual data permitted checks, comparisons, and corroborations of electric fabric interpretations. In the conductivity study the impedances of nine cores drilled in different directions (specified in Girdler, 1961) were determined in a two electrode water bath cell (Emerson, 1969) connected to an ESI AF Videobridge 2600 operating at 1 kHz. The specimens were vacuum saturated with 60 ohm.m (20°C) tap water. At the frequency used, measurement-electrode polarisation was minimal but the massive sulphide cores' termination impedances (at the core/water interface) were included in the measurement. This lead to lower conductivities than would be measured in situ or by laboratory inductive or four electrode techniques with very high impedance potential probes placed on the sulphide specimen surface. However, the two electrode method is quick and simple and appeared to provide reasonable relative conductivity values. Some details of the rock suites' characteristics are provided in Table 2. Differences between bulk 2.5 MHz electromagnetic/four electrode (as above) conductivities and two electrode galvanic conductivities (cited for the principal conductivity σ_1) are due to the differing responses of conducting minerals, imhomogeneities, and matrix materials, in irrotational electric fields and rotational magnetic field (Shaub, 1964) and/or termination impedance effects. A specially written HP41C program was used to calculate the principal values and principal directions of the conductivity tensor following the least squares procedure outlined by Hill (1972). Magnetic susceptibility principal axes were determined by a standard program in the Digico unit.

Results

The results for the shales and schists are presented in Table 3. Generally there is good agreement between the physical

SUSCEPTIBILITY ANISOTROPY

ANISOTROPY ELLIPSOIDS

$x^2/a^2+y^2/b^2+z^2/c^2 = 1$

magnetic k ellipsoid shown

RESPONSE = TENSOR x STIMULUS

$J_{mag} = k_{ij}F$

$J_{cd} = \sigma_{ij}E$

ELECTRICAL CONDUCTIVITY (σ) ELLIPSOID

substitute: σ_{ij} for k_{ij}, E for F, J_{cd} for J_{mag}

F magnetic field, E electric field, J_{mag} magnetisation, J_{cd} current density.

REPRESENTATION ELLIPSOID $k_1x^2+k_2y^2+k_3z^2 = 1$

DEFINITION

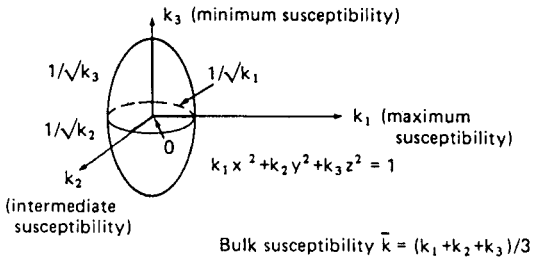

Bulk susceptibility $\bar{k} = (k_1+k_2+k_3)/3$

SUSCEPTIBILITY ELLIPSOID : MAGNETIC FABRIC

(not to be confused with representation ellipsoid)

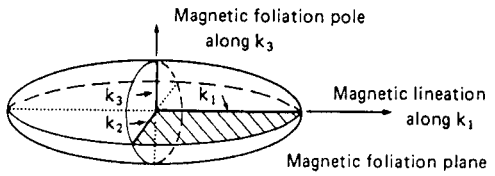

Anisotropy Magnitude $A = k_1/k_3$

Lineation Magnitude $L = k_1/k_2$

Foliation Magnitude $F = k_2/k_3$

Ellipsoid Prolateness $P = L/F$

- $P = 0$ uniaxial oblate ellipsoid (disc)
- $P = \infty$ uniaxial prolate ellipsoid (needle)

DEFLECTION OF MAGNETIZATION

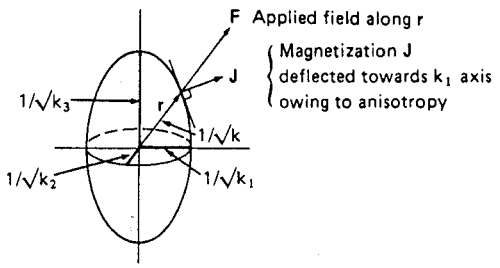

$k(r) = k_1l^2+k_2m^2+k_3n^2 = 1/r^2$

l,m,n = direction cosines of r

FIGURE 1
Magnetic and electrical anisotropy ellipsoids.

Symmetry	Tensor*	Ellipsoid Shape & Orientation	Fabric Elements Orientation	Examples (refer Fig. 2)
$K_{\infty h}$-spherical	$\begin{matrix} k_{11} & 0 & 0 \\ 0 & k_{11} & 0 \\ 0 & 0 & k_{11} \end{matrix}$	sphere	random	random equant grain aggregates lacking preferred orientation
$D_{\infty h}$-axial	$\begin{matrix} k_{11} & 0 & 0 \\ 0 & k_{11} & 0 \\ 0 & 0 & k_{33} \end{matrix}$	spheroid, rotational ellipsoid, revolution axis k_3// C	one ∞ fold axis// C	layered rocks
D_{2h}-orthorhombic	$\begin{matrix} k_{11} & 0 & 0 \\ 0 & k_{22} & 0 \\ 0 & 0 & k_{33} \end{matrix}$	triaxial ellipsoid, k_1// A, k_2// B, k_3// C	three 2-fold axes // A,B,C	layered and lineated rocks
C_{2h}-monoclinic	$\begin{matrix} k_{11} & k_{12} & 0 \\ k_{21} & k_{22} & 0 \\ 0 & 0 & k_{33} \end{matrix}$	triaxial ellipsoid, k_1,k_2 @ Λ A,B; k_3// C	one 2-fold axis // C	two intersecting planes (// strike) each with lineation
C_i-triclinic	$\begin{matrix} k_{11} & k_{12} & k_{13} \\ k_{21} & k_{22} & k_{23} \\ k_{31} & k_{32} & k_{33} \end{matrix}$	triaxial ellipsoid, k_1,k_2,k_3 @ Λ A,B,C	arbitrary	two obliquely intersecting planes each with lineation

* Tensor elements : magnetic susceptibility $k_{ij} = k_{ji}$, for electrical conductivity substitute $\sigma_{ij} = \sigma_{ji}$; other orientations (with respect to orthogonal fabric axes A,B,C) of the direction of the principal susceptibilities k_1,k_2,k_3 (or electrical conductivities $\sigma_1,\sigma_2,\sigma_3$) are possible.

Table 1. Second rank tensor symmetries.

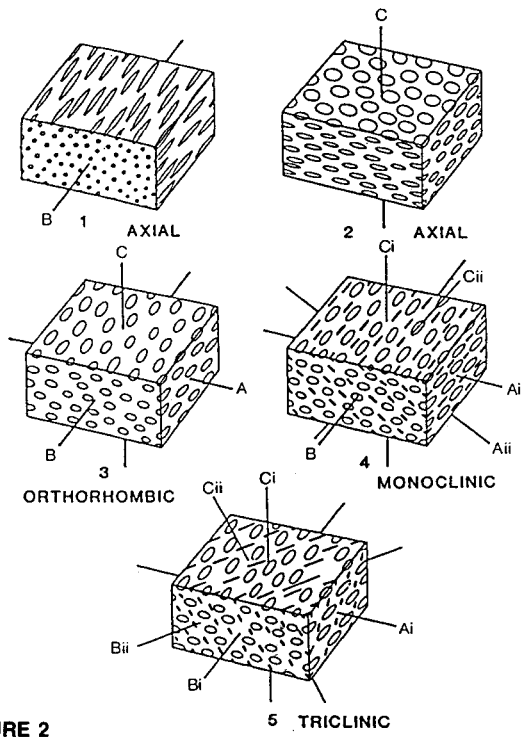

FIGURE 2
Examples of fabrics showing orthogonal fabric axes A, B, C (after F. J. Turner and L. E. Weiss, 1963, p. 89, Structural Analysis of Metamorphic Tectonites, McGraw-Hill).

properties and the petrofabrics. For sample No. 1 the relationship between petrofabric and the physical properties is unclear because of the low symmetry of the petrofabric. The electric fabric is probably influenced by both bedding and the vein systems. The magnetic fabric is weak, but appears to be well-defined and is probably a deformational fabric unrelated to the veining. In sample No. 24 the physical properties are consistent with the petrofabric. The electric fabric is sensitive only to the conductive pyritic layers and does not reflect the lineation defined by insulating minerals. The magnetic fabric appears to reflect the deformational fabric of the shaly layers, which biases the magnetic foliation away from the bedding plane towards the mineral lineation. In the schist specimen No. 14 there is reasonable agreement between electric fabric, magnetic fabric and petrofabric, with well-defined σ_3 and k_3 axes parallel to the bedding pole and less well-defined σ_1 and k_1 axes sub-parallel to the lineation. For schist specimens Nos. 16 and 23 there is excellent agreement between the electric fabric and the magnetic and petrofabrics.

Results

The results for the five sulphides are presented in Table 4. The fabrics are reasonably consistent in three cases, one case is indeterminate, and there is one poorly correlated case. For specimen No. 2 the electric and magnetic fabrics are reasonably concordant and the electric and magnetic lineations lie within the bedding plane, as expected. However, the physical properties are not consistent with the apparent foliation-dominant axial symmetry of the petrofabric suggesting that

Sample No., Lithology	Mineralogy	Observed Rock Texture			DBD	P_A	bulk σ	2 el.σ_{max}	σ_1/σ_3
		fol.	lin.	fabric	g/cc	%	s/m	s/m	A
BLACK SHALES (layered)									
1 Hellyer adit	1% py	✓		tri.	2.72	0.1	0.004	0.006	7.1
24 White Spur	7% py	✓	✓	mon.	2.58	1.8	0.012	0.030	v.large
QUARTZ, CHLORITE MUSCOVITE SCHISTS									
14 Prince Lyell	30% py, cpy	✓	✓	orth.	3.31	0.4	0.009	0.017	34.0
16 Prince Lyell	15% py, cpy	✓	✓	orth.	3.04	0.1	0.020	0.070	v.large
23 Cape Horn	2% py, cpy	✓	✓	orth.	2.81	0.4	0.007	0.015	v.large
SULPHIDES									
2 Que R. P lens	70%, b, py, sphal, qtz + gal, cpy	✓		axial	3.92	0.7	1.5	0.2	2.4
7 Tasman/Crown Lyell extended	95%, b, py, sphal + qtz, gal	✓		axial	4.44	2.4	1.0	0.1	2.9
8 West Lyell open cut	70% m, py, + qtz veins	✓		mon.	4.15	2.1	3.3	0.2	3.1
9 West Lyell open cut	50%, b, py + qtz	✓		axial	3.81	0.6	31.0	0.2	33.0
10 The Blow	80%, b, py	✓		axial	4.61	1.8	4.2	0.1	4.2

Notes: b=banded, m=massive, mineralogy approximate only; tri.=triclinic, mon.=monoclinic, orth.=orthorhombic; DBD=dry bulk density g/cc (t/m^3), P_A=apparent porosity %, DBD & P_A values average of 9 samples; bulk σ from lab. em 2.5 MHz inductive measurements (sulphides) or a four electrode galvanic technique (others); all samples have weak to very weak magnetic susceptibilities ≤ 100 x 10^{-6} cgs. (1257 x 10^{-6} SI); A=σ_1/σ_3 electrical anisotropy magnitude from interpreted conductivity ellipsoid principal axes, σ_3 minimum, where ratio 'very large' σ_1 well defined but σ_3 very small and difficult to quantify.

Table 2. Characteristics of Palaeozoic rocks and ores from Mt. Lyell and other areas, Tasmania.

Sample	Lithology	Characteristics	Petrofabric	Electric Fabric	Magnetic Fabric
1 (Hellyer Mine adit)	Fine-grained bedded black shale with two distinct systems of calcite/chlorite veins, both oblique to bedding	Fabric symmetry:	Triclinic	~Axial (slightly ortho-rhombic)	Orthorhombic
		Dominant fabric elements:	3 intersecting foliations (bedding, major veins, minor veins)	Foliation	Lineation
		Major axis:	~Parallel to intersection of 2 major foliations	~25° from intersection of vein systems	Unrelated to bedding or vein systems
		Intermediate axis:	⊥ major and minor axes	In bedding plane	
		Minor axis:	Between poles to two major foliations	~20° from bedding pole	
2 (White Spur)	Pyritic shale, with pyrite concentrated in thin layers parallel to bedding. Within shale layers there is a lineation, oblique to bedding, defined by quartz with phyllosilicate over-growths	Fabric symmetry:	Monoclinic	~Axial (slightly ortho-rhombic)	Orthorhombic
		Dominant fabric elements:	Lineation oblique to foliation (bedding)	Foliation	Foliation
		Major axis:	Projection of lineation onto bedding plane	Within bedding	~25° from bedding (towards lineation?)
		Intermediate axis:	2-fold symmetry axis within bedding plane	Within bedding	Within bedding (parallel to symmetry axis)
		Minor axis:	Pole to some plane, between lineation and bedding	Bedding pole	~25° from bedding pole
14 (Prince Lyell)	Quartz/chlorite/sericite schist (bedded pyro-clastic) with disseminated pyrite/ chalcopyrite + sulphide veins	Fabric symmetry:	Orthorhombic	Orthorhombic	Orthorhombic
		Dominant fabric elements:	Lineation within foliation (bedding)	Foliation	Foliation
		Major axis:	Lineation of clasts	Sub-parallel to lineation	Sub-parallel to lineation
		Intermediate axis:	In bedding plane, ⊥ lineation	~ ⊥ lineation, in bedding plane	~ ⊥ lineation, in bedding plane
		Minor axis:	Bedding pole	Parallel to bedding pole	Parallel to bedding pole
16 (Prince Lyell)	Quartz/chlorite/muscovite schist with disseminated and veined pyrite and chalcopyrite. The mineralisation is rodded within the schistosity	Fabric symmetry:	Orthorhombic	Orthorhombic	Orthorhombic
		Dominant fabric elements:	Lineation within foliation	Lineation	Lineation
		Major axis:	Lineation	Parallel to lineation	Parallel to lineation
		Intermediate axis:	⊥ lineation, in schistosity plane	⊥ lineation, in schistosity plane	⊥ lineation in schistosity plane
		Minor axis:	Schistosity pole	Schistosity pole	Schistosity pole
23 (Cape Horn)	Mineralised quartz/ chlorite/sericite schist with rodded pyrite and chalcopyrite within the schistosity	Fabric symmetry:	Orthorhombic	Orthorhombic	Orthorhombic
		Dominant fabric elements:	Lineation with foliation	Foliation	Lineation
		Major axis:	Lineation	Parallel to lineation	Parallel to lineation
		Intermediate axis:	⊥ lineation, in schistosity plane	⊥ lineation, in schistosity plane	⊥ lineation, in schistosity plane
		Minor axis:	Schistosity pole	Schistosity pole	Schistosity pole

Table 3. Fabrics — black shales and mineralised schists.

there is an undetected foliation intersecting the bedding at 90°. The results from No. 7 show reasonable agreement between electric and magnetic fabrics, which conform to the geometric fabric but suggest the presence of an undetected petrofabric lineation within the bedding. In sample No. 8 the magnetic fabric is too weak to determine accurately. The electric fabric axes do not bear any relationship to the geometric fabric and cannot be readily interpreted. The conductivity anisotropy suggests an undetected fabric within the massive pyrite. Electric fabric agrees well with petrofabric in sample No. 9 but suggests an undetected lineation within the pyrite layers. The magnetic fabric is very weak but the axes are apparently well-defined, although discordant with the petrofabric/electric fabric. In sample No. 10 the electric conductivity and magnetic susceptibility are too isotropic to give meaningful fabric elements.

Discussion

Overall the results are considered to be quite good. It is possible that better results could be obtained for the sulphides by employing a conductivity measuring technique designed to operate directionally on one sample (as for magnetic anisotropy) rather than measuring nine closely drilled but different cores with a two electrode technique. The data suggest that Palaeozoic rocks from mineralized areas may be characterized by strongly anisotropic electrical conductivities, knowledge of which may be useful in rock texture studies in exploration terrain.

Magnetic anisotropy needs to be considered in magnetic modelling of causative bodies with highly anisotropic susceptibilities. Equations incorporating anisotropy have been published by Emerson *et al.* (1985) and Clark *et al.* (1986).

The directional consequences of electrical anisotropy are usually ignored. $\tilde{E}$ and $\tilde{J}_{cd}$ are usually not collinear with $\tilde{J}_{cd}$ being deflected towards the easy conductivity direction. Consider the case of a bedded rock, similar to sample No. 9, with $\sigma_1:\sigma_2:\sigma_3$ = 33:16:1; σ_1 and σ_2 are in the plane of the layering, σ_3 is normal to the layering, and σ_1 is enhanced owing to rodded mineralization. An $\tilde{E}$ field applied across the diagonal of a unit cube of the material will have an inclination of 35° to the σ_1 σ_2 plane and a declination of 045° (relative to the σ_1 direction regarded as I = 0°, D = 0°. A current density vector will be produced in the direction D = 26°, I = −2°, not along the diagonal but at an angle of 38° to the diagonal; the current swings markedly towards the highest conductivity. Clearly tensor effects need to be taken into account in the relevant field equations for operations over anisotropic rocks.

It should be noted that this electrical study was concerned with micro-anisotropy observable in small specimens. In the field macro-anisotropy due to large scale layering would also need to be considered.

Sample	Lithology	Characteristics	Petrofabric	Electric Fabric	Magnetic Fabric
2 (Que River P lens)	Banded sulphide ore (pyrite /sphalerite/qtz + muscovite, galena, chalcopyrite)	Fabric symmetry:	Axial	~Axial (slightly ortho-rhombic)	Axial
		Dominant fabric elements:	Foliation	Lineation	Lineation
		Major axis:	In bedding plane	In bedding plane	Near bedding plane, close to major conductivity axis
		Intermediate axis:	In bedding plane	Near bedding plane	Not well-defined
		Minor axis:	Bedding pole	Near bedding plane	Not well-defined
7 (Tasman/Crown Lyell extended)	Banded sulphide ore (pyrite/sphalerite + quartz, galena)	Fabric symmetry:	Axial	~Axial (slightly ortho-rhombic)	~Axial (slightly orthorhombic)
		Dominant fabric elements:	Foliation	Foliation	Lineation
		Major axis:	In bedding plane	In bedding plane	In bedding plane near σ_1 axis
		Intermediate axis:	In bedding plane	In bedding plane	In bedding plane near σ_2 axis
		Minor axis:	Bedding pole	Parallel to bedding pole	Sub parallel to bedding pole
8 (W. Lyell Open Cut)	Massive pyrite with two quartz vein systems	Fabric symmetry:	Monoclinic(two-fold axis along inter-section of vein systems)	Orthorhombic	Spherical (isotropic)
		Dominant fabric elements:	Intersecting foliations + 2 foliations + lineation	Foliation	-
		Major axis:	Intersection of vein systems	~45° from lineation	-
		Intermediate axis:	⊥ lineation, between two foliations	~45° from lineation	-
		Minor axis:	Intermediate between poles to two vein systems	~45° from pole to major vein system, ~90° from pole to minor vein system	-
9 (W. Lyell Open Cut)	Banded sulphide ore with alternating pyritic and quartz layers	Fabric symmetry:	Axial	~Axial (slightly ortho-rhombic)	Orthorhombic
		Dominant fabric elements:	Foliation	Foliation	Lineation
		Major axis:	In bedding plane	In bedding plane	~In bedding plane
		Intermediate axis:	In bedding plane	In bedding plane	~In bedding plane
		Minor axis:	Bedding pole	Parallel to bedding pole	~30° from bedding pole
10 (The Blow)	Fine grained banded sulphide predominantly pyrite "massive" in appearance but grain size banded	Fabric symmetry:	Axial	~Spherical (isotropic)	~Spherical (isotropic)
		Dominant fabric elements:	Foliation	-	-
		Major axis:	In bedding plane	-	-
		Intermediate axis:	In bedding plane	-	-
		Minor axis:	⊥ In bedding plane	-	-

Table 4. Fabrics — sulphide and ores.

References

Bhathal, R. S. (1971)—'Magnetic anisotropy in rocks', *Earth Sci. Rev.* **7**, 227–253.

Clark, D. A., Saul, S. J. & Emerson, D. W. (1986)—'Magnetic and gravity anomalies of a triaxial ellipsoid', *Explor. Geophys.* **17**, 189–200.

Emerson, D. W. (1969)—'Laboratory electrical resistivity measurements of rocks', *Proc. Austral. Inst. Min. & Metall.* **230**, 51–62.

Emerson, D. W., Clark, D. A. & Saul, S. J. (1985)—'Magnetic exploration models incorporating remanence, demagnetization, and anisotropy: HP 41C handheld computer algorithms', *Explor. Geophys.* **16**, 1–122.

Hill, D. G. (1972)—'A laboratory investigation of electrical anisotropy in Precambrian rocks', *Geophysics* **37**, 1022–1038.

Hrouda, F. (1973)—'A determination of the symmetry of the ferromagnetic mineral fabric in rocks on the basis of the magnetic susceptibility anisotropy measurements', *Gerlands Beitr. Geophysik*, Leipzig B2, **5**, 390–396.

Kerr, T. L. (1986)—'Electrical anisotropy in sulphides and black shales — the determination and interpretation of the second order electrical conductivity tensor. B.Sc. Hons. thesis unpub. 2 vols. Department Geol. & Geophys. Uni. Sydney.

Noltimier, H. C. (1971)—'Determining magnetic anisotropy of rocks with a spinner magnetometer giving in-phase and quadrature data output', *Jour. Geophy. Res.* **76**, 4849–4854.

Nye, J. F. (1957)—'Physical Properties of Crystals', Oxford, Clarendon Press, 322 pp.

Shaub, Y. B. (1964)—'Measurement of rock resistivity in alternating electrical and magnetic fields', *Izv. Geophys. Ser.* 1964, No. 10, 1522–1526.

Turner, F. J. & Weiss, L. E. (1963)—'Structural Analysis of Metamorphic Tectonites', McGraw-Hill, 545 pp.

Girdler, R. W. (1961)—'The measurement and computation of anisotropy of magnetic susceptibility of rocks', *Geophys. Jour. Roy. Astron. Soc.* **5**, 34–44.